Role of syntaxin 18 in the organization of endoplasmic reticulum subdomains

Takayuki Iinuma[1], Takehiro Aoki[1], Kohei Arasaki[1,*], Hidenori Hirose[1], Akitsugu Yamamoto[2], Rie Samata[2], Hans-Peter Hauri[3], Nagisa Arimitsu[1], Mitsuo Tagaya[1] and Katsuko Tani[1,‡]

[1]School of Life Sciences, Tokyo University of Pharmacy and Life Sciences, Hachioji, Tokyo 192-0392, Japan
[2]Department of Bio-science, Nagahama Institute of Bio-science and Technology, Nagahama, Shiga 526-0829, Japan
[3]Department of Pharmacology and Neurobiology, Biozentrum, University of Basel, Basel CH-4056, Switzerland

*Present address: Section of Microbial Pathogenesis, Yale University School of Medicine, Boyer Center for Molecular Medicine, 295 Congress Avenue, New Haven, CT 06536, USA
‡Author for correspondence (e-mail: Tani@ls.toyaku.ac.jp)

Accepted 9 February 2009
Journal of Cell Science 122, 1680-1690 Published by The Company of Biologists 2009
doi:10.1242/jcs.036103

Summary

The presence of subdomains in the endoplasmic reticulum (ER) enables this organelle to perform a variety of functions, yet the mechanisms underlying their organization are poorly understood. In the present study, we show that syntaxin 18, a SNAP (soluble NSF attachment protein) receptor localized in the ER, is important for the organization of two ER subdomains, smooth/rough ER membranes and ER exit sites. Knockdown of syntaxin 18 caused a global change in ER membrane architecture, leading to the segregation of the smooth and rough ER. Furthermore, the organization of ER exit sites was markedly changed concomitantly with dispersion of the ER-Golgi intermediate compartment and the Golgi complex. These morphological changes in the ER were substantially recovered by treatment of syntaxin-18-depleted cells with brefeldin A, a reagent that stimulates retrograde membrane flow to the ER. These results suggest that syntaxin 18 has an important role in ER subdomain organization by mediating the fusion of retrograde membrane carriers with the ER membrane.

Supplementary material available online at
http://jcs.biologists.org/cgi/content/full/122/10/1680/DC1

Key words: Brefeldin A, COPII, Endoplasmic reticulum, Membrane fusion, Subdomain, Syntaxin 18

Introduction

The endoplasmic reticulum (ER) in mammalian cells is a reticular tubular network that extends from the nucleus to the cell periphery along the microtubule track. Although ER membranes constantly undergo fission and fusion, this organelle maintains a structure consisting of several distinct subdomains (for reviews, see Borgese et al., 2006; Levine and Rabouille, 2005; Shibata et al., 2006; Vedrenne and Hauri, 2006). The smooth ER is responsible for Ca^{2+} storage, lipid synthesis and drug detoxication. The rough ER has ribosomes and is involved in coupling protein synthesis to protein translocation into the lumen through the translocon consisting of the Sec61 complex. In the lumen of the ER, newly synthesized proteins undergo folding and post-translational modification. Correctly folded or assembled proteins are exported from the ER through a specified subdomain named transitional ER or ER exit sites, which are marked by the presence of the coat protein complex II (COPII) coat (Gürkan et al., 2006; Hammond and Glick, 2000).

Syntaxins are a family of soluble NSF attachment protein receptor (SNARE) proteins implicated in membrane fusion (Hong, 2005; Jahn and Scheller, 2006). Mammalian syntaxin members involved in transport between the ER and Golgi are syntaxin 5 and syntaxin 18, which are localized in the Golgi and the ER, respectively (Dascher et al., 1994; Hatsuzawa et al., 2000). Syntaxin 17 has been reported to be localized in the smooth ER, but its expression is limited to certain cell types such as steroidogenic cell types (Steegmaier et al., 2000). We have previously shown that syntaxin 18 forms a complex with three SNAREs (BNIP1/Sec20, p31/Use1 and Sec22b) and three peripheral membrane proteins (Sly1, ZW10 and RINT1) (Hirose et al., 2004; Nakajima et al., 2004). Syntaxin 18 is most probably the mammalian orthologue of yeast Ufe1 implicated in retrograde transport from the Golgi to the ER (Lewis and Pelham, 1996) and homotypic ER membrane fusion (Patel et al., 1998), because they are similar in amino acid sequence and form complexes of similar composition (Hirose et al., 2004; Kraynack et al., 2005; Nakajima et al., 2004). Our functional analysis suggested that two peripheral syntaxin-18-binding proteins, ZW10 and RINT1, are involved in transport between the ER and Golgi complex (Arasaki et al., 2006; Arasaki et al., 2007; Hirose et al., 2004), and that BNIP1 participates in the formation of the three-way junctions of the ER network (Nakajima et al., 2004). Recent studies demonstrated that syntaxin 18 and p31 also participate in phagocytosis and post-Golgi transport (Hatsuzawa et al., 2006; Okumura et al., 2006). The versatile ability of the syntaxin 18 complex may be related to a unique mechanism of SNARE core assembly (Aoki et al., 2008).

In the present study, we investigated the role of syntaxin 18 using RNA interference. Our results suggest that syntaxin 18 plays a key role in the organization of the smooth/rough ER and ER exit sites.

Results

Knockdown of syntaxin 18 induces ER membrane aggregation and Golgi disassembly

To examine the function of syntaxin 18, we knocked down its expression in HeLa cells using two short interfering RNAs (siRNAs). Immunoblotting showed that the expression level of syntaxin 18 was reduced markedly by Syn18(770) (Fig. 1A, left panel, lane 4) and more severely by Syn18(390) (lane 3) without a marked decrease in the expression of other proteins including components of the syntaxin 18 complex. Immunofluorescence analysis demonstrated that the intensity of syntaxin 18 staining was

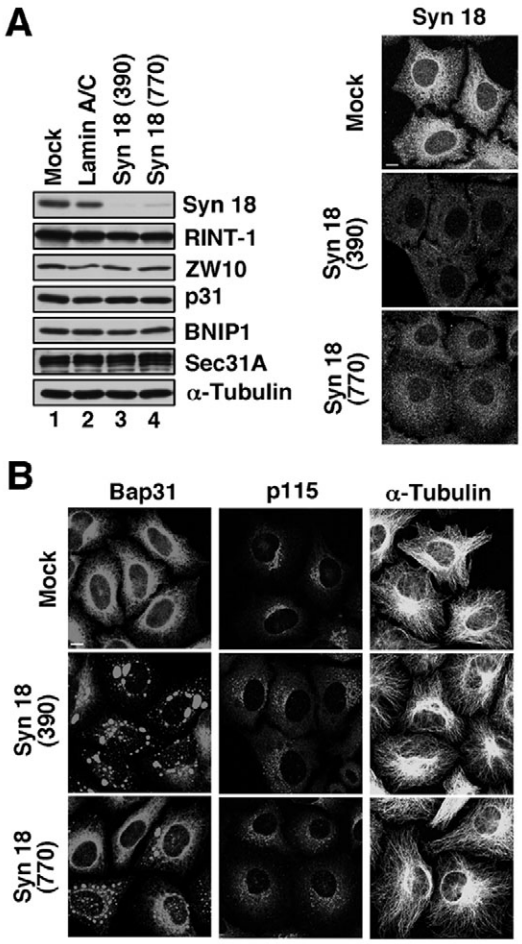

Fig. 1. Knockdown of syntaxin 18 induces ER membrane aggregation and disrupts the Golgi complex. (A) HeLa cells were mock-transfected or transfected with lamin A/C siRNA, Syn18(390) or Syn18(770). At 72 hours after transfection, the cells were stained with an antibody against syntaxin 18 (right) or solubilized in phosphate-buffered saline with 0.5% SDS. The lysates (10 μg each) were separated by SDS-PAGE and analyzed by immunoblotting with the indicated antibodies (left). (B) HeLa cells were treated as described in A and stained for Bap31, p115 or α-tubulin. The distributions of the proteins investigated were indistinguishable between mock-transfected cells and lamin A/C siRNA-treated cells (data not shown). Scale bars: 10 μm.

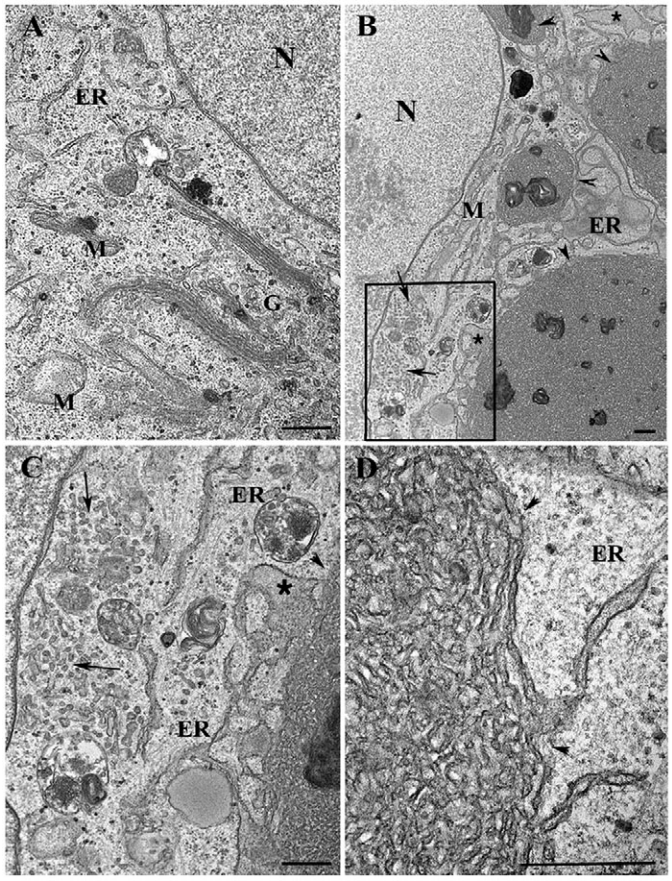

Fig. 2. Ultrastructure of syntaxin-18-depleted cells. HeLa cells were mock-transfected or transfected with Syn18(390), incubated for 72 hours and processed for electron microscopy. (A) An electron micrograph of a mock-transfected cell. (B-D) Electron micrographs of Syn18(390)-transfected cells. The boxed area in B is shown enlarged in C. G, Golgi complex; M, mitochondria; ER, endoplasmic reticulum; N, nucleus. Arrows, arrowheads and asterisks indicate vesiculated membrane structures, ER patches and dilated ER, respectively. Scale bars: 500 nm.

decreased in most cells upon transfection with Syn180 (390) (Fig. 1A, right panel, middle) and Syn18(770) (bottom).

In Syn18(390)-transfected cells, we frequently (40-50% of cells at 72 hours after transfection) observed large patches positive for an ER membrane protein, Bap31 (Annaert et al., 1997) (Fig. 1B, middle row, left). Albeit much less frequently, similar patches were observed in cells transfected with the less efficient siRNA Syn18(770) (bottom row, left), suggesting that the redistribution of Bap31 is a consequence of syntaxin 18 depletion, and not a consequence of off target effect of Syn18(390). The different frequencies of the Bap31-positive patches are probably the result of the different knockdown efficiency of the two siRNAs. Fig. 1B also shows that silencing of syntaxin 18 causes a substantial dispersion of the Golgi complex marked by a cis-Golgi marker, p115 (Waters et al., 1992), without affecting microtubules. Other Golgi proteins, such as GM130, mannosidase II (Man II), β-COP and the KDEL receptor (KDEL-R), were also dispersed (supplementary material Fig. S1). The time course of morphological changes of the ER and Golgi structures concomitant with syntaxin 18 depletion is shown in supplementary material Fig. S2.

To investigate in detail the morphology of the ER and the Golgi complex in syntaxin-18-depleted cells, we performed electron microscopy. In Syn18(390)-transfected cells, vesiculated membrane structures, instead of the Golgi stacks, were observed at the perinuclear region (Fig. 2B,C; supplementary material Fig. S3). Furthermore, there were well-defined membrane aggregates consisting of a convoluted network of branching tubules, as well as dilated ER structures, in Syn18(390)-transfected cells (Fig. 2B-D; supplementary material Fig. S3). Similar results were obtained with Syn18(770)-transfected cells, although ER aggregates were observed only in some cells (data not shown). Quantitative analysis showed that the area and length of the ER normalized to the cytoplasmic area of Syn18(390)-transfected cells are higher than those of mock-transfected cells (Tables 1 and 2), suggesting a proliferation of the ER membrane concomitant with syntaxin 18 depletion.

Immunoelectron microscopy confirmed Golgi disassembly and the formation of ER membrane aggregates in syntaxin-18-depleted cells. In Syn18(390)-transfected cells, a cis-Golgi marker, p115, and

Table 1. Increase of ER area in syntaxin-18-depleted cells

	ER	Dilated ER*	Aggregates	ER + aggregates
Syn18(390)-transfected cells	9.84±0.80	4.51±0.25	6.24±2.68	16.08±2.34
Mock-treated cells	6.85±0.96	0.36±0.23	0	6.85±0.9

Values are percentage of area of ER (μm^2)/cytoplasm (μm^2). Results are from three independent experiments.
*Dilated ER is ER with luminal width larger than 250 nm.

Table 2. Increase of ER membrane length in syntaxin-18-depleted cells

	ER	Aggregates*	ER + aggregates
Syn18(390)-transfected cells	1.67±0.06	3.42±1.47	5.09±1.48
Mock-treated cells	2.03±0.39	0	2.03±0.39

Values are the length of membranes (μm)/cytoplasm (μm^2). Results are from three independent experiments.
*Length of membranes in aggregates was calculated from the length of membrane (μm)/aggregate area (μm^2); 54.8±5.4 (n=3).

a trans-Golgi marker, Vti1a (Xu et al., 1998), were found to be present in vesicular profiles (Fig. 3A,B), and Bap31 in membrane aggregates (Fig. 3C). The antibodies used specifically labeled the Golgi complex (anti-p115 and anti-Vti1a) and ER membranes (anti-Bap31) in control cells (supplementary material Fig. S4A-C).

Depletion of syntaxin 18 segregates smooth and rough ER membranes

As ER patches in syntaxin-18-depleted cells are similar to those of smooth ER tubules in hepatocytes and in phenyl-2-decanoyl-amino-3-morpholino-1-propanol (PDMP)-treated cells expressing GFP attached to the ER membrane through the cytochrome b_5 tail (GFP-CB5) (Sprocati et al., 2006), we analyzed the distribution of several ER proteins including those enriched in the rough ER. In Syn18(390)-transfected cells, distribution of calnexin, SERCA2 and reticulon 4 was patchy and they were colocalized with Bap31 in the patches (Fig. 4A,B). Of note, reticulon 4 is a smooth ER membrane-localized protein that participates in shaping the tubular ER (Voeltz et al., 2006). Luminal ER proteins (protein disulfide isomerase (PDI) and Hsp47) also accumulated in patches, but these patches and Bap31-positive ones were separate in the cytoplasm (Fig. 4C, upper two rows; Fig. 4D, top row). Strikingly, no marked concentration in certain areas was observed for CLIMP-63 (also known as CKAP4) and Sec61β, both of which are membrane proteins enriched in the rough ER (Klopfenstein et al., 1998; Shibata et al., 2006), and for BNIP1, a component of the syntaxin 18 complex (Hirose et al., 2004) (Fig. 4C, lower three rows; Fig. 4D, lower two rows). Immunoelectron microscopy demonstrated that CLIMP-63 is localized in both normal and dilated ER membranes, but largely excluded from membrane aggregates (Fig. 3D). This localization is in contrast to that of Bap31 (Fig. 3C). Immunoelectron microscopy also showed that Hsp47 and PDI are in the lumen of the ER, especially abundant in dilated ER, but not in membrane aggregates (Fig. 3E and data not shown). These results, taken together, suggest that loss of syntaxin 18 causes the separation of smooth and rough ER membranes.

Knockdown of syntaxin 18 disrupts ER exit sites

Disturbance of the ER structure does not always accompany Golgi disassembly. For example, overexpression and knockdown of BNIP1 cause ER aggregation and loss of the three way junctions of the ER network, respectively, but do not significantly affect the Golgi structure (Nakajima et al., 2004). To understand why Golgi disassembly occurred in syntaxin-18-depleted cells, we

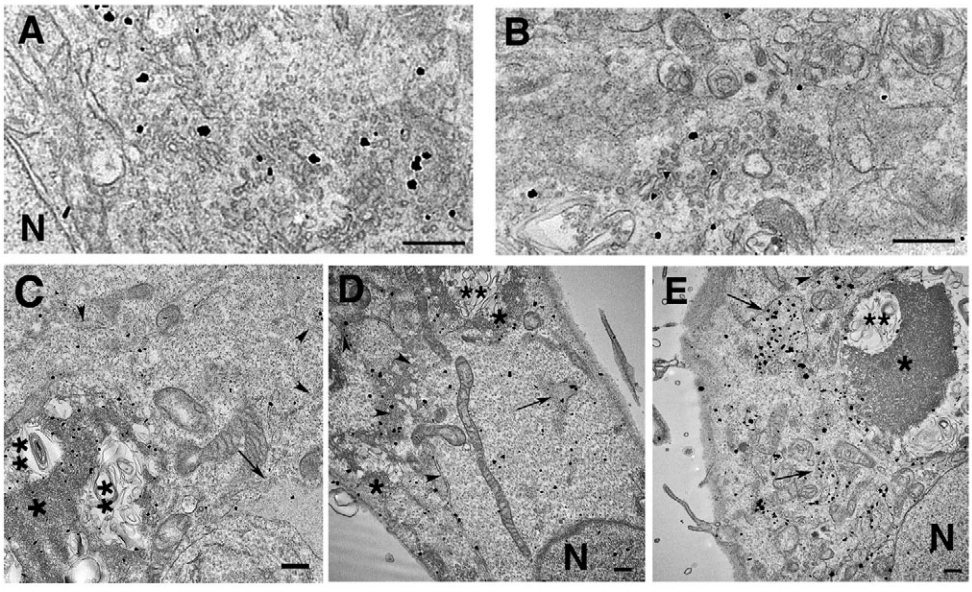

Fig. 3. Immunoelectron microscopy of ER and Golgi proteins in syntaxin-18-depleted cells. HeLa cells were transfected with Syn18(390), incubated for 72 hours and processed for immunoelectron microscopy. Localization of a cis-Golgi marker, p115 (A), a trans-Golgi marker, Vti1a (B), Bap31 (C), CLIMP-63 (D) and Hsp47 (E). N, nucleus. Arrowheads, arrows and asterisks indicate ER, dilated ER and ER patches, respectively. The structures labeled by double asterisks are incompletely fixed ER patches. Scale bars: 500 nm.

examined the distribution of marker proteins located in more proximal compartments in the early secretory pathway. As shown in Fig. 5A, knockdown of syntaxin 18 induced dispersion not only of an ER-Golgi intermediate compartment (ERGIC) marker, ERGIC-53 (also known as LMAN1) (Schweizer et al., 1988), but also of an ER exit site marker, Sec31A (Tang et al., 2000). In normal cells, Sec31A-positive puncta were distributed in the peripheral region with a significant concentration at the perinuclear area, whereas Sec31A-positive puncta did not accumulate at the perinuclear region in syntaxin-18-depleted cells (Fig. 5A, second column from the left). To substantiate the change of ER exit sites in syntaxin-18-depleted cells, cells were treated with 10 μg/ml nocodazole for 3 hours. Previous studies reported that when microtubules are depolymerized by nocodazole, Golgi and ERGIC proteins redistribute to the ER, leading to the proliferation of ER exit sites (Cole et al., 1996; Hammond and Glick, 2000; Storrie et al., 1998). As shown in Fig. 5B, in contrast to mock-transfected cells, nocodazole treatment did not result in substantial increase in the size of Sec31A-positive or ERGIC-53-positive dots in syntaxin-18-depleted cells. Similar results were obtained for other ER exit site markers, such as Sec16A (Bhattacharyya and Glick, 2007; Iinuma et al., 2007; Watson et al., 2006) and p125 (Shimoi et al., 2005).

Next, we examined whether disrupted ER exit sites in syntaxin-18-depleted cells remain functional, by measuring the transport from the ER of ts045 vesicular stomatitis virus-encoded glycoprotein attached to GFP (VSVG-GFP). For this purpose, we performed two consecutive transfections with Syn18(390) and the plasmid encoding VSVG-GFP, as described by Iinuma et al. (Iinuma et al., 2007). At the nonpermissive temperature, VSVG-GFP accumulated in smooth ER patches of Syn18(390)-transfected cells (supplementary material Fig. S5A, right panel, 0 minutes), consistent with the previous finding that VSVG can move from the rough ER to the smooth ER at the nonpermissive temperature (Bergmann and Fusco, 1990). After shift to the permissive temperature, it exited the ER and reached the plasma membrane through fragmented Golgi complex, with a time course not much different from that observed in mock-transfected cells. However, the acquisition of endoglycosidase H resistance by VSVG-GFP, a hallmark of its delivery to the medial Golgi, was slightly delayed (supplementary material Fig. S5B), implying that syntaxin 18 depletion slows down VSVG-GFP transport from the ER to the Golgi. Thus, ER exit sites in syntaxin-18-depleted cells are functional, but slightly less efficient for protein transport.

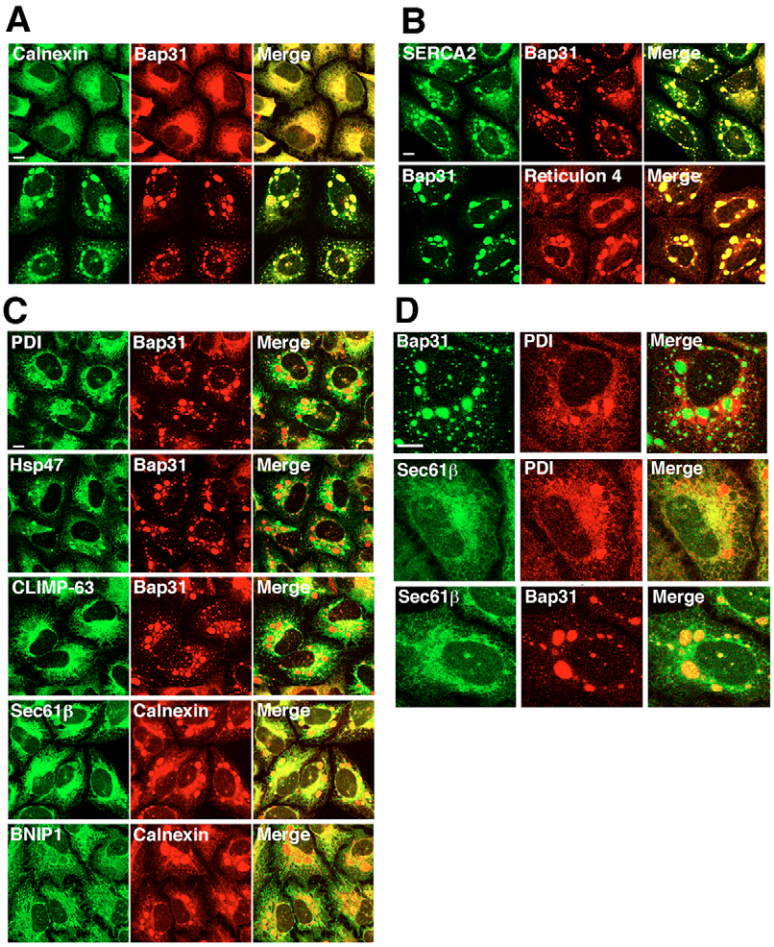

Fig. 4. Knockdown of syntaxin 18 results in segregation of smooth and rough ER membranes. (A) HeLa cells were mock-transfected (upper panels) or transfected with Syn18(390) (lower panels). At 72 hours after transfection, the cells were double-stained with antibodies against calnexin and Bap31. (B-D) HeLa cells transfected with Syn18(390) were double-stained with the indicated antibodies. A ×100 objective lens was used to obtain the images in D (A-C ×40). Scale bars: 10 μm.

Retrograde transport of ERGIC-53 to the ER appears to be blocked by depletion of syntaxin 18

It has been reported that the availability of cargo regulates the size of ER exit sites (Aridor et al., 1999; Forster et al., 2006; Guo and Linstedt, 2006; Heinzer et al., 2008). The inability of nocodazole to induce additional proliferation of ER exit sites in syntaxin-18-depleted cells may reflect a shortage of cycling components required for COPII assembly, which may be due to the inhibition of retrograde transport to the ER. To test this idea, we focused attention on the distribution of ERGIC-53. ERGIC-53 principally cycles between the ERGIC and ER in a COPI-dependent, but Rab6-independent manner (Girod et al., 1999; Nufer et al., 2002; Sun et al., 2007; White et al., 1999), thereby this protein is a good marker for the recycling pathway, although its loss does not block COPII assembly at ER exit sites (Mitrovik et al., 2008).

Although the overall staining intensity of ERGIC-53 was substantially increased in syntaxin-18-depleted cells (Fig. 5A, left column), this was not due to its upregulation, as demonstrated by immunoblotting (supplementary material Fig. S6A). The epitope of ERGIC-53 might be exposed by depletion of syntaxin 18 for an unknown reason. A similar phenomenon was observed when RINT1 expression was suppressed (Arasaki et al., 2006). When Syn18(390)-transfected cells were observed by immunofluorescence microscopy using a 100× objective lens, instead of a 40× lens as used for the experiment shown in Fig. 5, ERGIC-53 appeared dispersed in a dot-like staining pattern, albeit still with high background staining (Fig. 6B, upper two panels). When the distribution of GFP-ERGIC-53 (Ben-Tekaya et al., 2005) was examined, a similar dispersed pattern

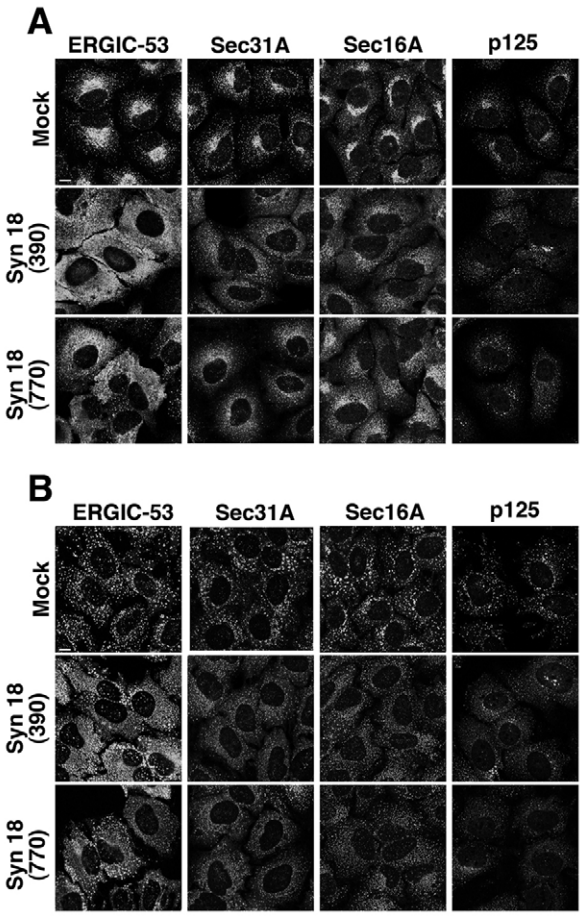

Fig. 5. ER exit sites are disorganized in syntaxin-18-depleted cells. HeLa cells were mock-transfected or transfected with Syn18(390) or Syn18(770), incubated for 72 hours and stained with the indicated antibodies immediately (A) or after incubation with 10 μg/ml nocodazole for 3 hours (B). Scale bars: 10 μm.

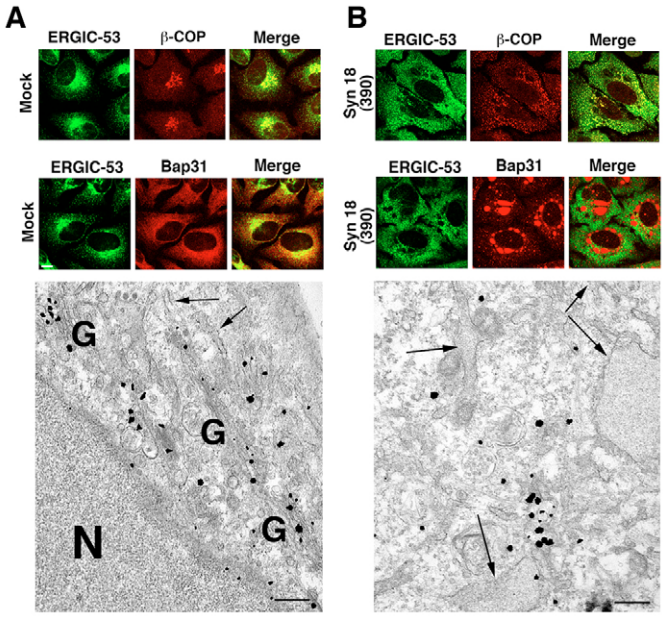

Fig. 6. ERGIC-53 is not returned to the ER in syntaxin-18-depleted cells. HeLa cells were mock-transfected (A) or transfected with Syn18(390) (B), incubated for 72 hours, double-stained with antibodies against ERGIC-53 and β-COP (top panel) or Bap31 (middle panel), and analyzed by immunofluorescence microscopy using a ×100 objective lens (upper two panels; scale bars: 10 μm). Alternatively, the cells were immunolabeled with ERGIC-53 and analyzed by electron microscopy (bottom panel; scale bars: 500 nm). N, nucleus; G, Golgi complex. Arrows indicate ER or dilated ER. Immunoreactivity of ERGIC-53 was observed near the Golgi in mock-transfected cells (A, bottom panel), whereas little, if any, ERGIC-53 immunoreactivity was detected in ER or dilated ER structures in Syn18(390)-transfected cells (B, bottom panel).

but with much lower background staining was observed (supplementary material Fig. S6B). It is noteworthy that many ERGIC-53-positive dots were also labeled by an anti-β-COP antibody (Fig. 6B, top panel), suggesting that ERGIC-53 is not retuned to the ER. Consistent with this idea, ERGIC-53 was not detected in smooth ER aggregates labeled by Bap31 in syntaxin-18-depleted cells (Fig. 6B, middle panel). Immunoelectron microscopy confirmed that ERGIC-53 is distributed in membranes throughout the cytoplasm but does not significantly accumulate at ER, dilated ER or ER aggregates in cells transfected with Syn18(390) (Fig. 6B, bottom panel; supplementary material Fig. S7).

Consistent with the previous finding that the transport of ERGIC-53 is regulated by COPI, but not Rab6 (Girod et al., 1999; Nufer et al., 2002), redistribution of ERGIC-53 caused by syntaxin 18 knockdown was not affected by the suppression of Rab6 expression (supplementary material Fig. S8C). By contrast, redistribution of Man II, for which the transport to the ER is regulated by Rab6 (Girod et al., 1999; White et al., 1999), was markedly blocked by depletion of Rab6 (supplementary material Fig. S8D).

To demonstrate that the diffuse ERGIC-53 distribution in syntaxin-18-depleted cells represents the nontethered and/or unfused state of COPI-coated membrane carries implicated in retrograde transport of ERGIC-53, cells were permeabilized with digitonin. A previous study showed that nontethered COG-complex-dependent Golgi vesicles are efficiently washed away from cells permeabilized with digitonin (Zolov and Lupashin, 2005). As shown in Fig. 7A, second row, the staining intensity of ERGIC-53 in mock-transfected cells was not markedly changed upon permeabilization. In contrast, the staining intensity of ERGIC-53 in Syn18(390)-transfected cells was substantially decreased (Fig. 7B, second row). However, the decrease in the intensity of Sec61β staining on permeabilization was not significantly different between mock- and Syn18(390)-transfected cells, although permeabilization caused some decrease in the intensity of Sec61β staining (Fig. 7A,B, second row). These results strongly suggest that ERGIC-53-positive membrane structures in syntaxin-18-depleted cells are not tightly associated with cellular structures in contrast to those in mock-transfected cells.

Defect in retrograde transport of VSVG-KDEL-R-YFP to the ER

To examine whether retrograde transport to the ER is impaired in syntaxin-18-depleted cells, we used a ts045 VSVG-KDEL-R chimera. At the permissive temperature (32°C), this chimera is localized in the cis-Golgi, and, upon shift to the nonpermissive temperature (40°C), it redistributes to the ER through the retrograde pathway (Cole et al., 1998; Yang et al., 2005). As reported previously (Yang et al., 2008), VSVG-KDEL-R-YFP, when expressed at 32°C, was localized in the perinuclear region in many

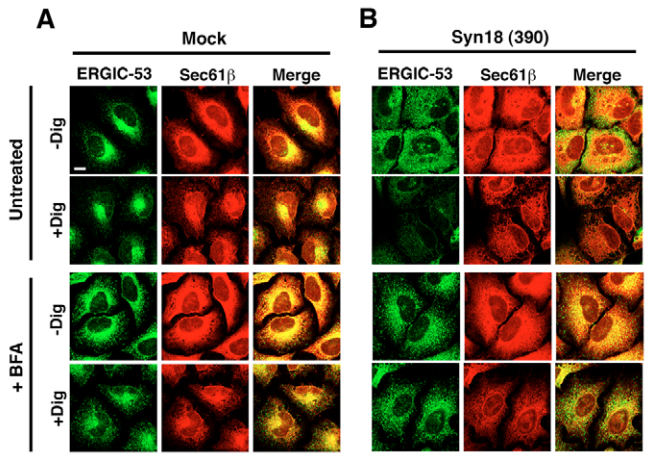

Fig. 7. Digitonin sensitivity of ERGIC-53 in syntaxin-18-depleted cells. HeLa cells were mock-transfected (A) or transfected with Syn18(390) (B). At 72 hours after transfection, the cells were left untreated or incubated with 10 µM BFA for 30 minutes, permeabilized with digitonin and double-stained with antibodies against ERGIC-53 and Sec61β. Scale bars: 10 µm.

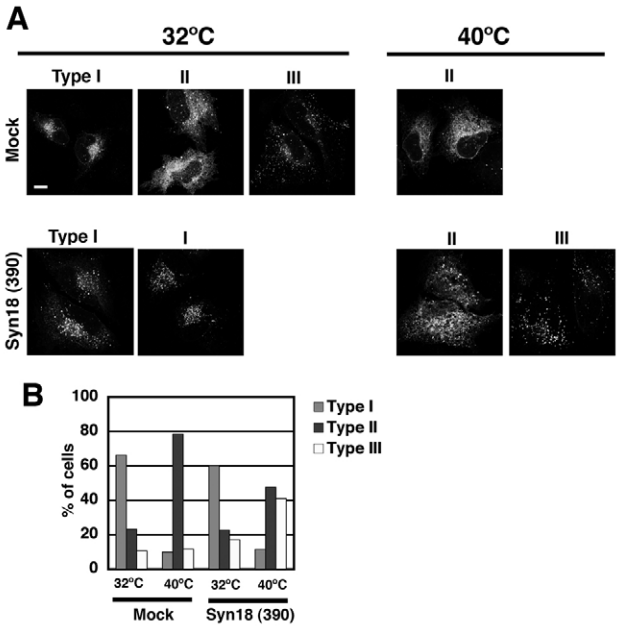

Fig. 8. Retrograde transport of VSVG-KDEL-R-YFP to the ER is inhibited by syntaxin 18 depletion. HeLa cells were mock-transfected or transfected with Syn18(390) and treated as described in Materials and Methods. The cells incubated at 32°C were fixed immediately (32°C) or incubated at 40°C for 2 hours before fixation (40°C). (A) VSVG-KDEL-R-YFP was concentrated in the perinuclear region as punctate structures (type I), localized in the ER with some in punctate structures (type II) or distributed as punctate structures throughout the cytoplasm (type III). Scale bar: 10 µm. (B) Quantification of the results. The average of two independent experiments is shown. For each sample, more than 200 cells were evaluated.

mock-transfected cells (Fig. 8A, top panel; classified here as type 1). In some cells, however, VSVG-KDEL-R-YFP was localized in the ER with some in punctate structures (type II) or distributed as punctate structures throughout the cytoplasm (type III). Fig. 8B shows the quantification of the results. Incubation of cells at 40°C for 2 hours induced redistribution of VSVG-KDEL-R-YFP to the ER (Fig. 8A, top right panel, type II, and Fig. 8B). Although VSVG-KDEL-R-YFP-positive punctate structures were localized in the perinuclear region of Syn18(390)-transfected cells at the nonpermissive temperature, their distribution was more diffuse than those in mock-transfected cells (Fig. 8A, type I, bottom versus top). Incubation of cells at 40°C for 2 hours less efficiently induced redistribution of VSVG-KDEL-R-YFP to the ER. In about 40% of cells, VSVG-KDEL-R-YFP-positive puncta were distributed diffusely throughout the cells (type III; Fig. 8B). These results suggest that the retrograde transport of VSVG-KDEL-R-YFP to the ER is inhibited by syntaxin 18 depletion.

Brefeldin A (BFA) treatment of syntaxin-18-depleted cells regenerates ER exit sites

Given that redistribution of ERGIC-53 is not regulated by Rab6, but probably mediated by COPI, we wondered whether the release of COPI from membranes may overcome the block of fusion of ERGIC-53-containing membranes with the ER. To test this idea, syntaxin-18-depleted cells were treated with BFA. BFA promotes Golgi disassembly by releasing COPI from Golgi and ERGIC membranes (Lippincott-Schwartz and Liu, 2006), but does not markedly disrupt peripheral ER exit sites (Shimoi et al., 2005; Ward et al., 2001). Upon BFA treatment, Golgi enzymes and ERGIC-53 redistribute to the ER and accumulate at peripheral ER exit sites, whereas cis-Golgi matrix proteins may move directly to ER exit sites (Mardones et al., 2006; Ward et al., 2001). Therefore, if factors that regulate the formation of ER exit sites are returned to the ER by BFA, it should be possible to observe COPII-positive dot-like structures in the peripheral region. Before BFA treatment, Sec31A exhibited a diffuse staining pattern in Syn18(390)-transfected cells (Fig. 9A, second row). Upon incubation with 10 µM BFA for 30 minutes, Sec31A accumulated in clear punctate structures (Fig. 9A, bottom row). In parallel, ERGIC-53 became colocalized with Sec31A in peripheral puncta, which were not stained by anti-Bap31 (Fig. 9A,B, bottom row). The redistribution of ERGIC-53 appeared to be the result of its recycling to the ER because ERGIC-53 staining was detected in ER aggregates (Fig. 9B, bottom row), as well as ER exit sites. Of note, ERGIC-53 staining in Syn18(390)-transfected cells was not diminished by digitonin treatment when the cells were pretreated with BFA (Fig. 7A,B, lower two rows), supporting the idea that ERGIC-53 redistributes to the ER upon BFA treatment. Redistribution of Golgi components to the ER in Syn18(390)-transfected cells was confirmed by the presence of the Golgi protein GPP130 (Linstedt et al., 1997) in the ER (supplementary material Fig. S9). These results suggest that BFA treatment induced the regeneration of ER exit sites in syntaxin-18-depleted cells by promoting the redistribution of components required for COPII assembly.

Because, in syntaxin-18-depleted cells, ER exit sites are regenerated by BFA treatment, we wondered whether ERGIC-53 in syntaxin-18-depleted cells might behave similarly to that in normal cells after BFA washout. To test this possibility, cells were incubated with BFA, washed to remove the reagent and further incubated for up to 3 hours. As reported previously (Lippincott-Schwartz et al., 1990; Saraste and Svensson, 1991; Wakana et al., 2008; Ward et al., 2001), BFA treatment of normal (mock-transfected) cells caused some loss of ERGIC-53-positive clusters at the perinuclear region without changing punctate ERGIC-53 staining at the peripheral region (supplementary material Fig. S10, left panel, second row). At 3 hours after BFA washout, ERGIC-53-

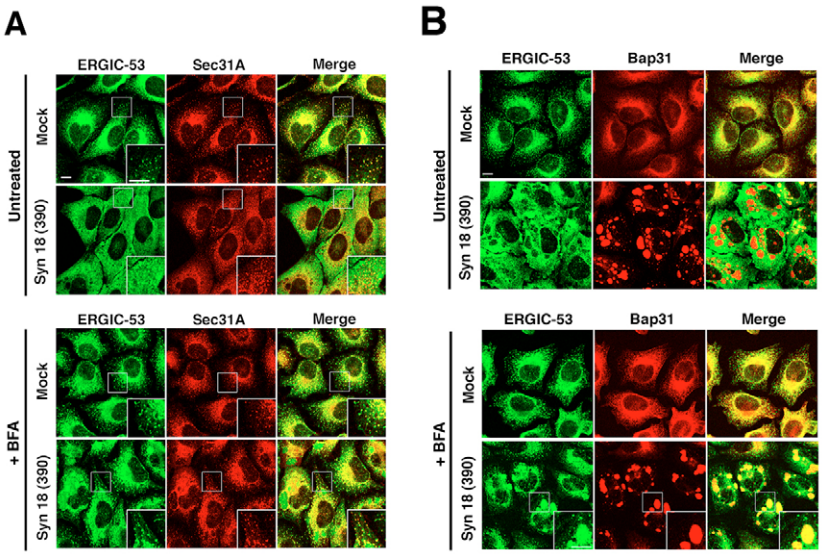

Fig. 9. Effect of BFA on the distribution of Sec31A and ERGIC-53 in syntaxin-18-depleted cells. HeLa cells were mock-transfected or transfected with Syn18(390). At 72 hours after transfection, the cells were left untreated or incubated with 10 μM BFA for 30 minutes and double-stained with antibodies against ERGIC-53 and Sec31A (A) or Bap31 (B). The boxed areas are shown enlarged in the insets. Scale bars: 10 μm.

positive clusters with some tubular structures accumulated at the perinuclear region in many cells (bottom row). During this BFA recovery process, substantial colocalization between ERGIC-53 and Sec31A was maintained in mock-transfected cells. In Syn18(390)-transfected cells, however, good colocalization between ERGIC-53 and Sec31A was gradually lost during incubation without BFA (supplementary material Fig. S10, right panel). At 3 hours after BFA washout, ERGIC-53 showed a diffuse staining pattern, similar to that observed before BFA treatment. These results may indicate that in syntaxin-18-depleted cells ERGIC-53 is not transported to regions distant from the ER, including the so-called ERGIC, upon removal of BFA, although ER exit sites are regenerated by BFA treatment.

BFA treatment of syntaxin-18-depleted cells regenerates the reticular ER structure

In the BFA experiments described above, we noticed that BFA treatment caused a decrease in the number of cells containing smooth ER patches. When counted using random images like those of Fig. 10A, the percentage of cells containing Bap31-positive patches was reduced from 45.2±2.6% to 9.8±1.9% upon BFA treatment for 30 minutes. By contrast, patches of luminal proteins, such as PDI, were not diminished by BFA treatment (Fig. 10B, right panel, middle column), indicating that the BFA effect is limited to the membrane structure. Loss of Bap31-positive patches indicates that segregation of smooth and rough ER membranes induced by depletion of syntaxin 18 can be at least partly reversed by BFA

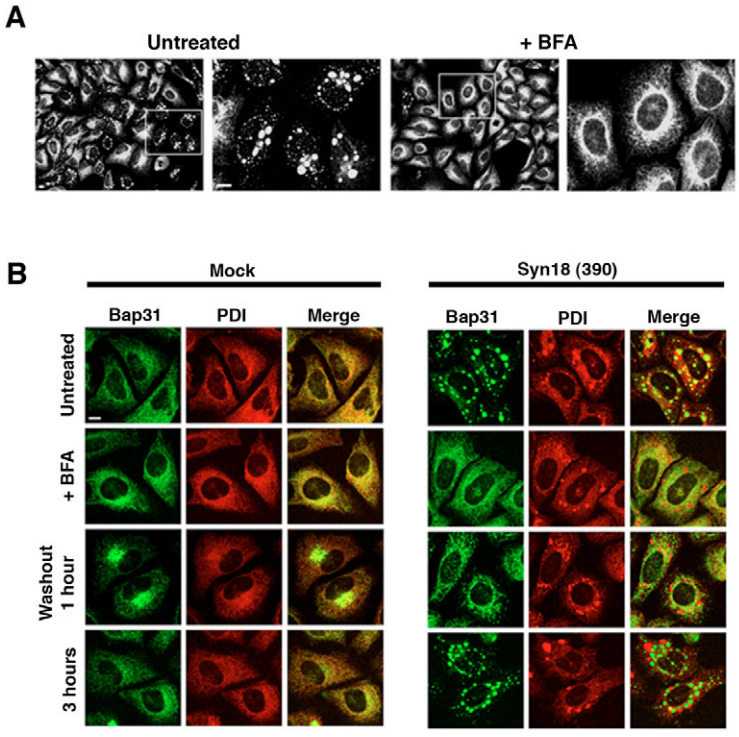

Fig. 10. BFA induces recovery of the ER architecture in syntaxin-18-depleted cells. (A) HeLa cells transfected with Syn18(390) were left untreated or treated with 10 μM BFA for 30 minutes, and then stained with an antibody against Bap31. The right panels of each pair are enlarged views of the boxed regions. (B) HeLa cells were treated as described in A. BFA was washed out, and the cells were incubated for the indicated times and double-stained with antibodies against Bap31 and PDI. Accumulation of Bap31 at the perinuclear region of mock-transfected cells at 1 hour after BFA washout may reflect its cycling within the ER during BFA recovery, as reported previously (Wakana et al., 2008). Scale bars: 10 μm.

treatment. As observed in the case of the localization of Sec31A and ERGIC-53 (supplementary material Fig. S10), the effect of BFA on ER membranes was reversible. ER patches were reformed by removal of BFA (Fig. 10B, right panel, left column).

Discussion

Yeast Ufe1 is involved in retrograde transport from the Golgi to the ER (Lewis and Pelham, 1996) and homotypic ER membrane fusion (Patel et al., 1998). In this study, we revealed that syntaxin 18, which is the probably mammalian orthologue of Ufe1, contributes to the organization of the smooth/rough ER domains and the formation of ER exit sites. The quantitative requirements of syntaxin 18 for these two functions seem to be different; formation of ER exit sites is more sensitive to the amount of syntaxin 18, whereas more complete knockdown of syntaxin 18 is necessary for the disruption of the ER architecture. Nevertheless, the defects in the two functions were substantially restored by BFA treatment.

Role of syntaxin 18 in the formation of ER exit sites

ER exit sites, which are coated by COPII coat, are immobile but dynamic (Gürkan et al., 2006; Hammond and Glick, 2000; Stephens, 2003). Recent studies have identified several proteins participating in the organization of ER exit sites. These include yeast and mammalian Sec16 (Bhattacharyya and Glick, 2007; Connerly et al., 2005; Iinuma et al., 2007; Watson et al., 2006), mammalian p125 (Shimoi et al., 2005) and *Drosophila* p115 (Kondylis and Rabouille, 2003), all of which are peripheral membrane proteins that accumulate at ER exit sites. In the present study, we showed that syntaxin 18 is required for the organization of ER exit sites in mammalian cells. Depletion of syntaxin 18 affected not only the spatial arrangement of ER exit sites but also their proliferation induced by nocodazole treatment. To our knowledge, this is the first case of the requirement of an integral ER membrane protein for the organization of ER exit sites.

To gain insight into the mechanism of how syntaxin 18 contributes to the organization of ER exit sites, we examined the behavior of ERGIC-53, a membrane protein that cycles between the ER and the ERGIC (Appenzeller-Herzog and Hauri, 2006). In syntaxin-18-depleted cells, ERGIC-53 was distributed in membranes dispersed throughout the cell, but with some local concentrations, inferred from a dot-like staining pattern with a high background. Immunoelectron microscopy showed that ERGIC-53 is not present in typical ER, dilated ER or smooth ER patches. BFA treatment resulted in the regeneration of ER exit sites concomitant with the relocalization of ERGIC-53 to ER exit sites. Perhaps not only ERGIC-53 but also other cycling membrane proteins could be redistributed to ER exit sites by BFA treatment, which allows COPII assembly by replenishing vesicle components. Mitrovic et al. (Mitrovic et al., 2008) recently investigated the role of cargo receptors, Sruf4, ERGIC-53 and a p24 family member, p25. Silencing of both Surf4 and ERGIC-53 or p25 results in Golgi disassembly and reduction in the number of ERGIC clusters, but does not affect ER exit sites. Therefore, cycling proteins other than ERGIC-53, Surf4 and p25 may be required for the formation of ER exit sites. Alternatively, a mass of cycling proteins and/or cargo, not specific proteins, may be required for the formation of ER exit sites.

The dispersed ERGIC-53 staining pattern in syntaxin-18-depleted cells may represent its presence in a subdomain of the ERGIC. A recent study showed that the ERGIC consists of different subdomains (marked by ERGIC-53 and Rab1), which were proposed to have different roles in anterograde and retrograde transport (Sannerud et al., 2006). In PC12 cells, BFA treatment results in missorting of p58 (rat ERGIC-53) to the tubular ERGIC domain and its transport to the neurites, where ER exit sites exist. BFA treatment of syntaxin-18-depleted cells might induce relocalization of ERGIC-53 to ER exit sites as a consequence of its retrograde transport to the ER or its redistribution within the subdomains of the ERGIC.

Although, in syntaxin-18-depleted cells, ER exit sites were regenerated by BFA treatment, ERGIC-53 (cargo) did not seem to be transported to distal compartments from the ER during recovery from BFA treatment. By contrast, VSVG-GFP (cargo) was exported from the ER and transported to the plasma membrane through disassembled Golgi membranes in syntaxin-18-depleted cells, although transport was somewhat delayed. This discrepancy between ERGIC-53 and VSVG-GFP is reminiscent of the recent finding by Stephens and colleagues that VSVG-YFP transport is not markedly affected by depletion of COPII components, the Sec13-Sec31 complex, whereas secretion of collagen is strongly impaired (Townley et al., 2008). Perhaps, VSVG is a very good cargo and may be capable of efficiently putting together machinery for its export from the ER even when expression levels of some machinery components are suppressed by RNA interference. Recent studies have shown that cargo itself regulates the rate of COPII assembly (Aridor et al., 1999; Forster et al., 2006; Guo and Linstedt, 2006; Heinzer et al., 2008). In the case of cargo proteins that have no or little, if any, potential to regulate COPII assembly, their exit from the ER may be impaired when the amounts of certain transport machinery components are reduced.

Role of syntaxin 18 in the organization of the smooth/rough ER

Knockdown of syntaxin 18 induced the formation of smooth ER patches, as well as dilated ER, concomitant with a proliferation of the ER membrane. Several ER membrane proteins were found to be principally localized in smooth ER aggregates, whereas rough ER proteins such as CLIMP-63 were largely excluded from these aggregates, but principally localized in normal and dilated ER, suggesting the segregation of smooth and rough ER membranes in syntaxin-18-depleted cells. Luminal proteins such as PDI and Hsp47 were abundantly present in dilated ER, but not in smooth ER patches. A previous study in yeast showed that Kar2p (BiP) and PDI are concentrated in a restricted region of the ER when anterograde or retrograde transport is blocked (Nishikawa et al., 1994). Therefore, the formation of PDI (Hsp47)-positive patches in syntaxin-18-depleted cells may reflect a partial defect in protein transport from and/or to the ER. Similar patches were observed when some components of the syntaxin 18 complex, other than syntaxin 18, were knocked down (Uemura et al., 2009) (and our unpublished data).

The structure of ER patches formed in syntaxin-18-depleted cells is quite similar to that observed when GFP-CB5-expressing cells are treated with PDMP (Sprocati et al., 2006). GFP-CB5, when expressed at moderate levels, causes a proliferation of ER membranes without affecting apparent ER morphology (Sprocati et al., 2006), whereas its high level overexpression results in the formation of stacked smooth cisternae (organized smooth ER) (Snapp et al., 2003). Although PDMP is known as an inhibitor of sphingolipid synthesis, its action on ER morphology is not related to this effect, but probably to the perturbation of calcium homeostasis (Sprocati et al., 2006). In this context, it is worth

mentioning that PDMP blocks BFA action, i.e. promotion of Golgi disassembly and subsequent retrograde transport of Golgi components to the ER, by affecting calcium homeostasis, not by inhibiting sphingolipid synthesis (Kok et al., 1998). Therefore, the formation of smooth ER patches in GFP-CB5-expressing cells by PDMP may be ascribable to its inhibitory action on retrograde transport through perturbation of calcium homeostasis. This morphological change in the ER induced by PDMP treatment of GFP-CB5-expressing cells and depletion of syntaxin 18 may reflect the importance of retrograde transport to the ER in the organization of the smooth/rough ER domains.

In the context of the role of syntaxin 18 as an ER organizing protein, it is interesting that the ER has a second syntaxin, syntaxin 17, which is abundant in steroidogenic cells and is probably involved in smooth ER membrane dynamics (Steegmaier et al., 2000). Although most syntaxins and other SNAREs have a C-terminal transmembrane domain of 17-25 amino acids with a short luminal tail following the α-helical SNARE motif (Hong, 2005), syntaxin 17 has at the C-terminal region two consecutive hydrophobic domains (~25 and 15 amino acids in length, respectively) separated by a single lysine, followed by 33 charged and uncharged residues (Steegmaier et al., 1998). This structural motif is remarkably different from that of syntaxin 18, which has a 17-amino-acid transmembrane domain followed by a five-amino-acid luminal tail. It is expected that such long consecutive hydrophobic regions of syntaxin 17 can form a hairpin structure in the membrane. Rapoport and colleagues (Shibata et al., 2006; Voeltz et al., 2006) suggested that proteins having an unusual hairpin topology in membranes can stabilize membrane curvature, thereby allowing the formation of tubules, which are characteristics of smooth ER membranes. It will be interesting to investigate in future studies whether the C-terminal hydrophobic region of syntaxin 17 forms a hairpin structure in membranes and plays a role in stabilizing the tubular ER structure.

It was unexpected that the phenotype of cells depleted of syntaxin 18 is markedly different from that of cells depleted of BNIP1 (yeast Sec20 orthologue), because the two proteins form a quaternary SNARE complex with Sec22b and p31 (yeast Use1) (Hirose et al., 2004). Loss of BNIP1 abrogates the three-way junctions of the ER network (Nakajima et al., 2004). This disrupted ER is similar to that observed in cells where p97-p47- or p97-p37-mediated fusion is blocked (Kano et al., 2005a; Kano et al., 2005b; Uchiyama et al., 2002; Uchiyama et al., 2006). p97, also known as VCP, is the mammalian orthologue of yeast Cdc48 that forms a complex with Ufe1 (Patel et al., 1998). Although Kano et al. (Kano et al., 2005a) claimed that p97 can interact through p47 with GST-syntaxin 18 lacking the transmembrane domain in vitro, our immunoprecipitation and pull-down experiments using cell lysates failed to detect the presence of a p97-p47-syntaxin 18 complex (data not shown). Because of the similar ER morphology of cells lacking BNIP1 and p97 activity, it is tempting to speculate that BNIP1, not syntaxin 18, is involved in the p97-mediated ER membrane fusion pathway.

Materials and Methods

Antibodies

A monoclonal antibody against syntaxin 18 and polyclonal antibodies against syntaxin 18, p31, BNIP1, RINT1, ZW10, Bap31, p125 and Sec16A were produced as described (Arasaki et al., 2006; Hatsuzawa et al., 2000; Hirose et al., 2004; Iinuma et al., 2007; Nakajima et al., 2004; Tani et al., 1999; Wakana et al., 2008). Polyclonal antibodies against Sec31A, β-COP and Bap31 were prepared in this laboratory. Monoclonal antibodies against ERGIC-53 and CLIMP-63 were prepared as described previously (Schweizer et al., 1993; Schweizer et al., 1988). A monoclonal antibody against p115 and a polyclonal antibody against the KDEL-R were generous gifts from M. Gerard Waters (Merck Research Laboratories, Rahway, NJ) and Hans-Dieter Söling (Max-Planck-Institute, Göttingen, Germany), respectively. Monoclonal antibodies against calnexin, Vti1a and p115 were obtained from BD Transduction Laboratories. Monoclonal antibodies against α-tubulin, PDI, Hsp47 and SERCA2 were obtained from Sigma-Aldrich, Daiichi Fine Chemical, Stressgen and Calbiochem, respectively. Polyclonal antibodies against Man II, Sec61β and GPP130 were purchased from Chemicon, Upstate Biotechnology and Covance, respectively. A goat anti-reticulon 4 antibody and a rabbit anti-Rab6 antibody were purchased from Santa Cruz Biotechnology.

Cell culture and plasmid transfection

HeLa cells were cultured in Eagle's minimum essential medium supplemented with 50 IU/ml penicillin, 50 μg/ml streptomycin and 10% fetal calf serum. Transfection of plasmids into cells was performed using LipofectAMINE PLUS reagent (Invitrogen) according to the manufacturer's protocol.

Immunofluorescence microscopy

Immunofluorescence microscopy was performed as described previously (Tagaya et al., 1996). Cells were fixed with methanol at –20°C for 5 minutes for staining of syntaxin 18 and BNIP1, or with 4% paraformaldehyde at room temperature for 20 minutes for other proteins. Confocal images were obtained using an Olympus Fluoview 300. Unless otherwise stated, a 40× objective lens was used.

Conventional electron microscopy

Conventional electron microscopy was performed as described previously (Yamaguchi et al., 1997). HeLa cells were cultured on plastic coverslips (Celldesk LF1, Sumitomo Bakelite) and were fixed with 2.5% glutaraldehyde (Electron Microscopy Sciences) in 0.1 M sodium phosphate buffer, pH 7.4 (PB), for 2 hours. After washing with distilled water, the specimens were postfixed in 1% OsO_4 containing 1.5% potassium ferrocyanide in PB for 60 minutes at room temperature, and washed with distilled water. The specimens were dehydrated in a series of graded ethanol solutions and embedded in epoxy resin. Ultra-thin sections were observed under an H7600 electron microscope (Hitachi).

For quantitative analyses, electron micrographs were taken at a magnification of 10,000×. Ten cell profiles were taken in each experiment, and three independent experiments were performed. In syntaxin-18-depleted cells, only the cells containing smooth ER aggregates were analyzed. The length of the ER membrane, the area of the ER compartment and the area of cytoplasm were measured using the software MacSCOPE 2.5 (Mitani Corporation, Fukui, Japan). As it is difficult to measure the length of the membrane composing smooth ER aggregates, we calculated aggregate membrane length from the area of aggregate and the average value of membrane length/area of aggregate: 54.8±5.4 μm/μm^2 (n=3). This value was obtained by measuring the total membrane length and the area of three aggregates at a magnification of 50,000×.

Immunoelectron microscopy

The pre-embedding gold enhancement immunogold method was used for immunoelectron microscopy, as described previously (Wakana et al., 2008). Briefly, cells were cultured on plastic coverslips and were fixed in 4% paraformaldehyde in PB for 2 hours at room temperature. After permeabilization in PB containing 0.25% saponin for 30 minutes followed by blocking for 30 minutes in PB containing 0.1% saponin, 10% bovine serum albumin, 10% normal goat serum and 0.1% cold water fish skin gelatin, the cells were exposed overnight to rabbit or mouse primary antibodies in the blocking solution. The specimens were incubated with colloidal gold (1.4 nm in diameter, Nanoprobes, New York, NY)-conjugated goat anti-rabbit IgG or mouse-IgG in the blocking solution for 2 hours, and the signal was intensified with a gold enhancement kit (GoldEnhance EM, Nanoprobes) for 3 minutes at room temperature. The specimens were post-fixed in 1% OsO_4 containing 1.5% potassium ferrocyanide and were processed for electron microscopy similarly to that for conventional electron microscopy.

RNA interference

siRNAs used for targeting were Syn18(770) (5′-aagggagagugguugagauuu-3′), Syn18(390) (5′-caggaccgcuguuuuggauuu-3′), Rab6 (5′-aagacatctttgatcaccaga-3′), which can knock down both Rab6a and Rab6a′ (Young et al., 2005) and lamin A/C (5′-ctggacttccagaagaacatt-3′). The siRNAs were purchased from Japan BioServices. HeLa cells were grown on 35-mm plates and transfected with siRNAs using OligofectAmine according to the manufacturer's protocol. Their final concentration was 100 nM. At 72 hours after transfection, the cells were processed for immunoblotting or immunofluorescence analysis.

VSVG-GFP transport assay

The plasmid encoding ts045 VSVG-GFP was kindly supplied by Jennifer Lippincott-Schwartz (NIH, Bethesda, MD). Experiments were conducted as described by Iinuma et al. (Iinuma et al., 2007).

Retrograde transport assay

The plasmid encoding ts045VSVG-KDEL-R-YFP was kindly supplied by Alberto Luini (Consorzio Mario Negri Sud, Italy). HeLa cells grown on 35-mm dishes were mock-transfected or transfected with Syn18(309) and incubated at 37°C for 48 hours. The cells were then transfected with 1 μg of the plasmid encoding VSVG-KDEL-R-YFP and incubated at 32°C for 24 hours. Cycloheximide was added to the medium at a final concentration of 20 μg/ml, and the cells were incubated for another 2 hours. To monitor retrograde transport, the temperature was shifted to 40°C. After 2 hours, the cells were fixed and processed for immunofluorescence analysis.

Digitonin permeabilization

HeLa cells were washed twice with permeabilization buffer (20 mM Hepes-KOH, pH 7.4, 50 mM NaCl, 2 mM $MgCl_2$, 250 mM sucrose and 1 mM dithiothreitol), and then incubated with 50 μg/ml digitonin (Merck) at 4°C for 20 minutes. The cells were washed twice with permeabilization buffer and processed for immunofluorescence microscopy.

This work was supported in part by Grants-in-Aid for Scientific Research (#18570186 and #18370081) from the Ministry of Education, Science, Sports, and Culture of Japan. We thank M. Gerard Waters, D. Hans-Dieter Söling, Jennifer Lippincott-Schwartz and Alberto Luini for gifts of reagents.

References

Annaert, W. G., Becker, B., Kistner, U., Reth, M. and Jahn, R. (1997). Export of cellubrevin from the endoplasmic reticulum is controlled by BAP31. *J. Cell Biol*. **139**, 1397-1410.

Aoki, T., Kojima, M., Tani, K. and Tagaya, M. (2008). Sec22b-dependent assembly of endoplasmic reticulum Q-SNARE proteins. *Biochem. J*. **410**, 93-100.

Appenzeller-Herzog, C. and Hauri, H. P. (2006). The ER-Golgi intermediate compartment (ERGIC): in search of its identity and function. *J. Cell Sci*. **119**, 2173-2183.

Arasaki, K., Taniguchi, M., Tani, K. and Tagaya, M. (2006). RINT-1 regulates the localization and entry of ZW10 to the syntaxin 18 complex. *Mol. Biol. Cell* **17**, 2780-2788.

Arasaki, K., Uemura, T., Tani, K. and Tagaya, M. (2007). Correlation of Golgi localization of ZW10 and centrosomal accumulation of dynactin. *Biochem. Biophys. Res. Commun*. **359**, 811-816.

Aridor, M., Bannykh, S. I., Rowe, T. and Balch, W. E. (1999). Cargo can modulate COPII vesicle formation from the endoplasmic reticulum. *J. Biol. Chem*. **274**, 4389-4399.

Ben-Tekaya, H., Miura, K., Pepperkok, R. and Hauri, H. P. (2005). Live imaging of bidirectional traffic from the ERGIC. *J. Cell Sci*. **118**, 357-367.

Bergmann, J. E. and Fusco, P. J. (1990). The G protein of vesicular stomatitis virus has free access into and egress from the smooth endoplasmic reticulum of UT-1 cells. *J. Cell Biol*. **110**, 625-635.

Bhattacharyya, D. and Glick, B. S. (2007). Two mammalian Sec16 homologues have nonredundant functions in endoplasmic reticulum (ER) export and transitional ER organization. *Mol. Biol. Cell* **18**, 839-849.

Borgese, N., Francolini, M. and Snapp, E. (2006). Endoplasmic reticulum architecture: structures in flux. *Curr. Opin. Cell Biol*. **18**, 358-364.

Cole, N. B., Sciaky, N., Marotta, A., Song, J. and Lippincott-Schwartz, J. (1996). Golgi dispersal during microtubule disruption: regeneration of Golgi stacks at peripheral endoplasmic reticulum exit sites. *Mol. Biol. Cell* **7**, 631-650.

Cole, N. B., Ellenberg, J., Song, J., DiEuliis, D. and Lippincott-Schwartz, J. (1998). Retrograde transport of Golgi-localized proteins to the ER. *J. Cell Biol.* **140**, 1-15.

Connerly, P. L., Esaki, M., Montegna, E. A., Strongin, D. E., Levi, S., Soderholm, J. and Glick, B. S. (2005). Sec16 is a determinant of transitional ER organization. *Curr. Biol*. **15**, 1439-1447.

Dascher, C., Matteson, J. and Balch, W. E. (1994). Syntaxin 5 regulates endoplasmic reticulum to Golgi transport. *J. Biol. Chem.* **269**, 29363-29366.

Forster, R., Weiss, M., Zimmermann, T., Reynaud, E. G., Verissimo, F., Stephens, D. J. and Pepperkok, R. (2006). Secretory cargo regulates the turnover of COPII subunits at single ER exit sites. *Curr. Biol*. **16**, 173-179.

Girod, A., Storrie, B., Simpson, J. C., Johannes, L., Goud, B., Roberts, L. M., Lord, J. M., Nilsson, T. and Pepperkok, R. (1999). Evidence for a COP-I-independent transport route from the Golgi complex to the endoplasmic reticulum. *Nat. Cell Biol*. **1**, 423-430.

Guo, Y. and Linstedt, A. D. (2006). COPII-Golgi protein interactions regulate COPII coat assembly and Golgi size. *J. Cell Biol*. **174**, 53-63.

Gürkan, C., Stagg, S. M., Lapointe, P. and Balch, W. E. (2006). The COPII cage: unifying principles of vesicle coat assembly. *Nat. Rev. Mol. Cell. Biol*. **7**, 727-738.

Hammond, A. T. and Glick, B. S. (2000). Dynamics of transitional endoplasmic reticulum sites in vertebrate cells. *Mol. Biol. Cell* **11**, 3013-3030.

Hatsuzawa, K., Hirose, H., Tani, K., Yamamoto, A., Scheller, R. H. and Tagaya, M. (2000). Syntaxin 18, a SNAP receptor that functions in the endoplasmic reticulum, intermediate compartment, and *cis*-Golgi vesicle trafficking. *J. Biol. Chem*. **275**, 13713-13720.

Hatsuzawa, K., Tamura, T., Hashimoto, H., Hashimoto, H., Yokoya, S., Miura, M., Nagaya, H. and Wada, I. (2006). Involvement of syntaxin 18, an endoplasmic reticulum (ER)-localized SNARE protein, in ER-mediated phagocytosis. *Mol. Biol. Cell* **17**, 3964-3977.

Heinzer, S., Wörz, S., Kalla, C., Rohr, K. and Weiss, M. (2008). A model for the self-organization of exit sites in the endoplasmic reticulum. *J. Cell Sci*. **121**, 55-64.

Hirose, H., Arasaki, K., Dohmae, N., Takio, K., Hatsuzawa, K., Nagahama, M., Tani, K., Yamamoto, A., Tohyama, M. and Tagaya, M. (2004). Implication of ZW10 in membrane trafficking between the endoplasmic reticulum and Golgi. *EMBO J*. **23**, 1267-1278.

Hong, W. (2005). SNAREs and traffic. *Biochim. Biophys. Acta* **1744**, 120-144.

Iinuma, T., Shiga, A., Nakamoto, K., O'Brien, M. B., Aridor, M., Arimitsu, N., Tagaya, M. and Tani, K. (2007). Mammalian Sec16/p250 plays a role in membrane traffic from the endoplasmic reticulum. *J. Biol. Chem*. **282**, 17632-17639.

Jahn, R. and Scheller, R. H. (2006). SNAREs: engines for membrane fusion. *Nat. Rev. Mol. Cell. Biol*. **7**, 631-643.

Kano, F., Kondo, H., Yamamoto, A., Kaneko, Y., Uchiyama, K., Hosokawa, N., Nagata, K. and Murata, M. (2005a). NSF/SNAPs and p97/p47/VCIP135 are sequentially required for cell cycle-dependent reformation of the ER network. *Genes Cells* **10**, 989-999.

Kano, F., Kondo, H., Yamamoto, A., Tanaka, A. R., Hosokawa, N., Nagata, K. and Murata, M. (2005b). The maintenance of the endoplasmic reticulum network is regulated by p47, a cofactor of p97, through phosphorylation by cdc2 kinase. *Genes Cells* **10**, 333-344.

Klopfenstein, D. R., Kappeler, F. and Hauri, H. P. (1998). A novel direct interaction of endoplasmic reticulum with microtubules. *EMBO J*. **17**, 6168-6177.

Kok, J. W., Babia, T., Filipeanu, C. M., Nelemans, A., Egea, G. and Hoekstra, D. (1998). PDMP blocks brefeldin A-induced retrograde membrane transport from golgi to ER: evidence for involvement of calcium homeostasis and dissociation from sphingolipid metabolism. *J. Cell Biol*. **142**, 25-38.

Kondylis, V. and Rabouille, C. (2003). A novel role for dp115 in the organization of tER sites in *Drosophila*. *J. Cell Biol*. **162**, 185-198.

Kraynack, B. A., Chan, A., Rosenthal, E., Essid, M., Umansky, B., Waters, M. G. and Schmitt, H. D. (2005). Dsl1p, Tip20p, and the novel Dsl3 (Sec39) protein are required for the stability of the Q/t-SNARE complex at the endoplasmic reticulum in yeast. *Mol. Biol. Cell* **16**, 3963-3977.

Levine, T. and Rabouille, C. (2005). Endoplasmic reticulum: one continuous network compartmentalized by extrinsic cues. *Curr. Opin. Cell Biol*. **17**, 362-368.

Lewis, M. J. and Pelham, H. R. B. (1996). SNARE-mediated retrograde traffic from the Golgi complex to the endoplasmic reticulum. *Cell* **85**, 205-215.

Linstedt, A. D., Mehta, A., Suhan, J., Reggio, H. and Hauri, H. P. (1997). Sequence and overexpression of GPP130/GIMPc: evidence for saturable pH-sensitive targeting of a type II early Golgi membrane protein. *Mol. Biol. Cell* **8**, 1073-1087.

Lippincott-Schwartz, J. and Liu, W. (2006). Insights into COPI coat assembly and function in living cells. *Trends Cell Biol*. **16**, e1-e4.

Lippincott-Schwartz, J., Donaldson, J. G., Schweizer, A., Berger, E. G., Hauri, H. P., Yuan, L. C. and Klausner, R. D. (1990). Microtubule-dependent retrograde transport of proteins into the ER in the presence of brefeldin A suggests an ER recycling pathway. *Cell* **60**, 821-836.

Mardones, G. A., Snyder, C. M. and Howell, K. E. (2006). Cis-Golgi matrix proteins move directly to endoplasmic reticulum exit sites by association with tubules. *Mol. Biol. Cell* **17**, 525-538.

Mitrovic, S., Ben-Tekaya, H., Koegler, E., Gruenberg, J. and Hauri, H. P. (2008). The cargo receptors Surf4, endoplasmic reticulum-Golgi intermediate compartment (ERGIC)-53 and p25 are required to maintain the architecture of ERGIC and Golgi. *Mol. Biol. Cell* **19**, 1976-1990.

Nakajima, K., Hirose, H., Taniguchi, M., Kurashina, H., Arasaki, K., Nagahama, M., Tani, K., Yamamoto, A. and Tagaya, M. (2004). Involvement of BNIP1 in apoptosis and endoplasmic reticulum membrane fusion. *EMBO J*. **23**, 3216-3226.

Nishikawa, S., Hirata, A. and Nakano, A. (1994). Inhibition of endoplasmic reticulum (ER)-to-Golgi transport induces relocalization of binding protein (BiP) within the ER to form the BiP bodies. *Mol. Biol. Cell* **5**, 1129-1143.

Nufer, O., Guldbrandsen, S., Degen, M., Kappeler, F., Paccaud, J. P., Tani, K. and Hauri, H. P. (2002). Role of cytoplasmic C-terminal amino acids of membrane proteins in ER export. *J. Cell Sci*. **115**, 619-628.

Okumura, A. J., Hatsuzawa, K., Tamura, T., Nagaya, H., Saeki, K., Okumura, F., Nagao, K., Nishikawa, M., Yoshimura, A. and Wada, I. (2006). Involvement of a novel Q-SNARE, D12, in quality control of the endomembrane system. *J. Biol. Chem*. **281**, 4495-4506.

Patel, S. K., Indig, F. E., Olivieri, N., Levine, N. D. and Latterich, M. (1998). Organelle membrane fusion: a novel function for the syntaxin homolog Ufe1p in ER membrane fusion. *Cell* **92**, 611-620.

Sannerud, R., Marie, M., Nizak, C., Dale, H. A., Pernet-Gallay, K., Perez, F., Goud, B. and Saraste, J. (2006). Rab1 defines a novel pathway connecting the pre-Golgi intermediate compartment with the cell periphery. *Mol. Biol. Cell* **17**, 1514-1526.

Saraste, J. and Svensson, K. (1991). Distribution of the intermediate elements operating in ER to Golgi transport. *J. Cell Sci*. **100**, 415-430.

Schweizer, A., Fransen, J. A., Bächi, T., Ginsel, L. and Hauri, H. P. (1988). Identification, by a monoclonal antibody, of a 53-kD protein associated with a tubulo-vesicular compartment at the *cis*-side of the Golgi apparatus. *J. Cell Biol*. **107**, 1643-1653.

Schweizer, A., Ericsson, M., Bächi, T., Griffiths, G. and Hauri, H. P. (1993). Characterization of a novel 63 kDa membrane protein. Implications for the organization of the ER-to-Golgi pathway. *J. Cell Sci*. **104**, 671-683.

Shibata, Y., Voeltz, G. K. and Rapoport, T. A. (2006). Rough sheets and smooth tubules. *Cell* **126**, 435-439.

Shimoi, W., Ezawa, I., Nakamoto, K., Uesaki, S., Gabreski, G., Aridor, M., Yamamoto, A., Nagahama, M., Tagaya, M. and Tani, K. (2005). p125 is localized in endoplasmic reticulum exit sites and involved in their organization. *J. Biol. Chem*. **280**, 10141-10148.

Snapp, E. L., Hegde, R. S., Francolini, M., Lombardo, F., Colombo, S., Pedrazzini, E., Borgese, N. and Lippincott-Schwartz, J. (2003). Formation of stacked ER cisternae by low affinity protein interactions. *J. Cell Biol*. **163**, 257-269.

Sprocati, T., Ronchi, P., Raimondi, A., Francolini, M. and Borgese, N. (2006). Dynamic and reversible restructuring of the ER induced by PDMP in cultured cells. *J. Cell Sci*. **119**, 3249-3260.

Steegmaier, M., Yang, B., Yoo, J. S., Huang, B., Shen, M., Yu, S., Luo, Y. and Scheller, R. H. (1998). Three novel proteins of the syntaxin/SNAP-25 family. *J. Biol. Chem*. **273**, 34171-34179.

Steegmaier, M., Oorschot, V., Klumperman, J. and Scheller, R. H. (2000). Syntaxin 17 is abundant in steroidogenic cells and implicated in smooth endoplasmic reticulum membrane dynamics. *Mol. Biol. Cell* **11**, 2719-2731.

Stephens, D. J. (2003). *De novo* formation, fusion and fission of mammalian COPII-coated endoplasmic reticulum exit sites. *EMBO Rep*. **4**, 210-217.

Storrie, B., White, J., Rottger, S., Stelzer, E. H., Suganuma, T. and Nilsson, T. (1998). Recycling of golgi-resident glycosyltransferases through the ER reveals a novel pathway and provides an explanation for nocodazole-induced Golgi scattering. *J. Cell Biol*. **143**, 1505-1521.

Sun, Y., Shestakova, A., Hunt, L., Sehgal, S., Lupashin, V. and Storrie, B. (2007). Rab6 regulates both ZW10/RINT-1- and conserved oligomeric Golgi complex-dependent Golgi trafficking and homeostasis. *Mol. Biol. Cell* **18**, 4129-4142.

Tagaya, M., Furuno, A. and Mizushima, S. (1996). SNAP prevents Mg^{2+}-ATP-induced release of *N*-ethylmaleimide-sensitive factor from the Golgi apparatus in digitonin-permeabilized PC12 cells. *J. Biol. Chem*. **271**, 466-470.

Tang, B. L., Zhang, T., Low, D. Y., Wong, E. T., Horstmann, H. and Hong, W. (2000). Mammalian homologues of yeast sec31p: an ubiquitously expressed form is localized to endoplasmic reticulum (ER) exit sites and is essential for ER-Golgi transport. *J. Biol. Chem*. **275**, 13597-13604.

Tani, K., Mizoguchi, T., Iwamatsu, A., Hatsuzawa, K. and Tagaya, M. (1999). p125 is a novel mammalian Sec23p-interacting protein with structural similarity to phospholipid-modifying proteins. *J. Biol. Chem*. **274**, 20505-20512.

Townley, A. K., Feng, Y., Schmidt, K., Carter, D. A., Porter, R., Verkade, P. and Stephens, D. J. (2008). Efficient coupling of Sec23-Sec24 to Sec13-Sec31 drives COPII-dependent collagen secretion and is essential for normal craniofacial development. *J. Cell Sci*. **121**, 3025-3034.

Uchiyama, K., Jokitalo, E., Kano, F., Murata, M., Zhang, X., Canas, B., Newman, R., Rabouille, C., Pappin, D., Freemont, P. et al. (2002). VCIP135, a novel essential factor for p97/p47-mediated membrane fusion, is required for Golgi and ER assembly *in vivo*. *J. Cell Biol*. **159**, 855-866.

Uchiyama, K., Totsukawa, G., Puhka, M., Kaneko, Y., Jokitalo, E., Dreveny, I., Beuron, F., Zhang, X., Freemont, P. and Kondo, H. (2006). p37 is a p97 adaptor required for Golgi and ER biogenesis in interphase and at the end of mitosis. *Dev. Cell* **11**, 803-816.

Uemura, T., Sato, T., Aoki, T., Yamamoto, A., Okada, T., Hirai, R., Harada, R., Mori, K., Tagaya, M. and Harada, A. (2009). p31 deficiency influences endoplasmic reticulum tubular morphology and cell survival. *Mol. Cell. Biol*. **29**, 1869-1881.

Vedrenne, C. and Hauri, H. P. (2006). Morphogenesis of the endoplasmic reticulum: beyond active membrane expansion. *Traffic* **7**, 639-646.

Voeltz, G. K., Prinz, W. A., Shibata, Y., Rist, J. M. and Rapoport, T. A. (2006). A class of membrane proteins shaping the tubular endoplasmic reticulum. *Cell* **124**, 573-586.

Wakana, Y., Takai, S., Nakajima, K. I., Tani, K., Yamamoto, A., Watson, P., Stephens, D. J., Hauri, H. P. and Tagaya, M. (2008). Bap31 is an itinerant protein that moves between the peripheral endoplasmic reticulum (ER) and a juxtanuclear compartment related to ER-associated degradation. *Mol. Biol. Cell* **19**, 1825-1836.

Ward, T. H., Polishchuk, R. S., Caplan, S., Hirschberg, K. and Lippincott-Schwartz, J. (2001). Maintenance of Golgi structure and function depends on the integrity of ER export. *J. Cell Biol*. **155**, 557-570.

Waters, M. G., Clary, D. O. and Rothman, J. E. (1992). A novel 115-kD peripheral membrane protein is required for intercisternal transport in the Golgi stack. *J. Cell Biol*. **118**, 1015-1026.

Watson, P., Townley, A. K., Koka, P., Palmer, K. J. and Stephens, D. J. (2006). Sec16 defines endoplasmic reticulum exit sites and is required for secretory cargo export in mammalian cells. *Traffic* **7**, 1678-1687.

White, J., Johannes, L., Mallard, F., Girod, A., Grill, S., Reinsch, S., Keller, P., Tzschaschel, B., Echard, A., Goud, B. et al. (1999). Rab6 coordinates a novel Golgi to ER retrograde transport pathway in live cells. *J. Cell Biol*. **147**, 743-760.

Xu, Y., Wong, S. H., Tang, B. L., Subramaniam, V. N., Zhang, T. and Hong, W. (1998). A 29-kilodalton Golgi soluble N-ethylmaleimide-sensitive factor attachment protein receptor (Vti1-rp2) implicated in protein trafficking in the secretory pathway. *J. Biol. Chem*. **273**, 21783-21789.

Yamaguchi, T., Yamamoto, A., Furuno, A., Hatsuzawa, K., Tani, K., Himeno, M. and Tagaya, M. (1997). Possible involvement of heterotrimeric G proteins in the organization of the Golgi apparatus. *J. Biol. Chem*. **272**, 25260-25266.

Yang, J. S., Lee, S. Y., Spanò, S., Gad, H., Zhang, L., Nie, Z., Bonazzi, M., Corda, D., Luini, A. and Hsu, V. W. (2005). A role for BARS at the fission step of COPI vesicle formation from Golgi membrane. *EMBO J*. **24**, 4133-4143.

Yang, J. S., Gad, H., Lee, S. Y., Mironov, A., Zhang, L., Beznoussenko, G. V., Valente, C., Turacchio, G., Bonsra, A. N., Du, G. et al. (2008). A role for phosphatidic acid in COPI vesicle fission yields insights into Golgi maintenance. *Nat. Cell Biol*. **10**, 1146-1153.

Young, J., Stauber, T., del Nery, E., Vernos, I., Pepperkok, R. and Nilsson, T. (2005). Regulation of microtubule-dependent recycling at the *trans*-Golgi network by Rab6A and Rab6A'. *Mol. Biol. Cell* **16**, 162-177.

Zolov, S. N. and Lupashin, V. V. (2005). Cog3p depletion blocks vesicle-mediated Golgi retrograde trafficking in HeLa cells. *J. Cell Biol*. **168**, 747-759.